95-130

ОБЪЕДИНЕННЫЙ
ИНСТИТУТ
ЯДЕРНЫХ
ИССЛЕДОВАНИЙ

Дубна

95-130

E9-95-130

I.N.Meshkov, A.N.Skrinsky*

ANTIHYDROGEN BEAM GENERATION USING STORAGE RINGS

Submitted to «Nuclear Instruments and Methods»

*Budker Institute of Nuclear Physics, 650090 Novosibirsk, Russia

1995

Introduction

The idea of antihydrogen atom generation appeared soon after realisation of the electron cooling method [1] and was developed since that time (see the bibliography in [2]). The main interest of antihydrogen production is not only philosophical one, as a generation of a simplest pieces of *antimatter*, but it has also some concrete goal - the test of CPT theorem in comparison of spectra of hydrogen and antihydrogen atoms.

This paper has the purpose to attract again an attention of high energy physic's community to a possibility of realisation of intense antihydrogen stream generation in the nearest future.

1. The general scheme

For antihydrogen atom generation an antiproton ring (LEAR in the case to be discussed) has to be supplied with additional one to store and to cool positrons (Fig.1). This ring has a focusing system with longitudinal magnetic field and therefore recombination of antiproton and positron in antihydrogen occurs in this field (p.2). Antihydrogen atoms are extracted through a vacuum channel to a spectrometric system for spectral measurements.

Both rings are equipped with electron cooling devices for cooling of antiprotons and positrons. It permits to receive dense $\overline{p}$ - beam and cold $\overline{p}$ and e^+ ones, to be recombined. The methods of positron generations are briefly discussed below (p.3).

A scheme with longitudinal magnetic field and completely immersed in it positron and electron beams has few advantages. First of all, such a scheme permits to achieve very strong and homogeneous focusing of positrons, applicable for wide range of position energy (Table 1 below). The second point is the possibility of use of traditional scheme for electron cooling (see p.p.4 and 5). At last, the reducing of the magnetic field in the positron source area and its compression in recombination and gun areas enables one to get more cold and dense positron beam and to enhance recombination rate (p.7).

The disadvantage of this scheme is, that positron beam size does not change during cooling procedure. There is a big temptation to place positron source outside solenoid [3] ("the Bush theorem"), to have a positron beam compression during cooling. However, transverse velocities of positrons are so high here, that electron cooling does not work productively. Therefore most effective way is to immerse a positron source (a target) in magnetic field, to accept positron beam emittance as high as possible and to use electron cooling for diminish of angular spread in the positron beam for receiving of high recombination rate.

The analysis shows, that the main practical limitation of the antihydrogen generation rate at LEAR is the lack of low energy positions (see p.3). The case of very intensive positron beam limited only by its space charge was discussed in [4,5].

For experiments with antihydrogen the low particle energy is preferable [6], therefore two cases are considered below - the $\overline{p}$ energy, conventional for LEAR - 50 MeV, and lowest energy, achievable at LEAR - 0.5 MeV.

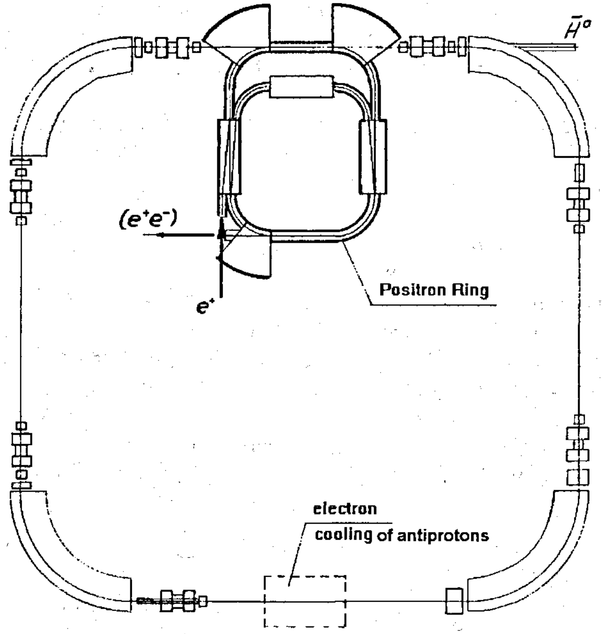

Fig.1. Layout of LEAR-complex with the Positron Ring

2. The recombination rate

The rate of $\overline{H^o}$ generation is described by formula

$$R \equiv \frac{dN}{dt} = \frac{1}{\gamma}\eta_p \alpha_r \cdot \frac{N_p N^+}{C^+ \pi a^2}, \quad a = \max\{a_p, a^+\}, \qquad (1)$$

where α_r is recombination coefficient [2,7]:

$$\alpha_r = \frac{20\alpha r_e^2 c^2 L_c}{V}, \qquad V = \sqrt{(V_p)^2 + (V^+)^2}, \qquad (2)$$

N_p, N^+ are antiproton and positron beams intensities, a_p, a^+ - the radii of their cross-sections, η_p - ratio of recombination region length to LEAR circumference,

C^+- the position ring circumference, V_p, V^+ - antiproton and positron velocities in the particle rest frame, $\alpha = 1/137$, r_e - the electron classical radius, $L_c = \ln(\alpha c / V)$, $\gamma = (1-\beta^2)^{-1/2}$, $\beta = v_o / c$, v_o-the average particle velocity in laboratory frame.

The standard LEAR storing, deceleration and cooling procedure permits to receive the beam at antiproton energy 50 MeV with the intensity about 10^{10} particles and the emittance $\pi\varepsilon \sim 3\pi$ mm·mrad [8]. One can hope, that $\overline{\text{p}}$-beam intensity can be increased up to $1\cdot 10^{11}$ with $\varepsilon_V \approx \varepsilon_H \approx 0.5\pi$ mm·mrad. It corresponds to $V_p \sim 3\cdot 10^6$ cm/s and $a_p \sim 1.5$ mm.

The optimal scheme parameters correspond, obviously, to equal transverse dimensions of positron and antiproton beams

$$a = a_p = a^+, \qquad (3)$$

when no "spare" particles are circulating in both rings. The positron velocities V^+ in cooled positron beam are at least of order of electron transverse velocities in the cooling electron beam, if the intensity of the positron beam is low enough. Thus, $V^+ \sim \sqrt{2T_\perp / m} \sim 3\cdot 10^7$ cm/s and does not depend strongly on particle energy (because electron transverse temperature $T_\perp$ is defined mainly by cathode temperature). Therefore one can neglect with V_p in formula (2). The achievable values of R are presented in Table 1.

Table 1.

The recombination rate with cooled $\overline{p}$- and e^+- beams

$\overline{p}$-beam energy, MeV intensity radius, mm	50 $1\cdot 10^{11}$ 1.5	0.5 $1\cdot 10^{9}$ 1.5
e^+-beam energy, keV intensity	27.2 $1\cdot 10^{9}$	0.27 $1\cdot 10^{8}$
C^+, m	21.56	21.56
η_p	0.02	0.02
$\overline{H}^0$ generation rate, atoms/sec	$1\cdot 10^{4}$	25

3. The positron source

The problem of low energy positron production constitutes the main limitation of $\overline{H}^0$ generation rate. Three methods of production of such positrons are known now:

1) a linear accelerator with electron beam, bombarding a target at electron energy about 40 MeV; positrons, produced in the depth of the target, travels to its surface and decelerate [6,9,10];

2) a source of the hard synchrotron radiation with photon energy above the pair generation threshold [11];

3) a strong radioactive source [12].

Table 2

The comparison of slow positron sources

Primary particle	e^-	γ	A^*
Primary particle energy, MeV	40	1.2	---
Conversion efficiency $N^+ / N_{e,\gamma}$	$1 \cdot 10^{-7}$	$3 \cdot 10^{-5}$	1
Available e^+ flux, $\sec^{-1}$	$1 \cdot 10^8$	$2 \cdot 10^{12}$	$1 \cdot 10^6$

The very attractive (see Table 2) is the second method, but it seems unrealizable at CERN facility dislocation. The 3-d method has obvious disadvantage of high radioactivity in use.

The energy spread of positrons, emitted by the target, is few eV, and one can accelerate they up to chosen energy ε_0, if to put the target under corresponding positive potential. After such electrostatic acceleration positron longitudinal momentum spread, and longitudinal temperature in particle rest frame reduce significantly, however transversal temperature conserves and has the same value T_t as at the target (see Ref. [5]):

$$T_{\parallel} = \frac{T_s^2}{2\varepsilon_0}, \quad T_{\perp} = T_t \sim 1 \text{ eV}. \tag{4}$$

To decrease the last one, one can use electron cooling [3].

4. The electron cooling of positrons. A general description

The use of electron cooling of positrons is the first decisive peculiarity of this proposal. It can be described with the same well known formulae [1], what are used for heavy particle electron cooling, if to substitute in it the electron (positron!) mass instead proton (ion) one and to add in the dominator factor 2, taking into account "technical" (reduced) mass of electron-positron colliding particles (see Ref.[3]):

$$\tau_{ee} = \frac{\beta^4 \cdot \gamma^5}{8\pi c r_e} \cdot \frac{mc^3}{\eta_e e J_e} \cdot \frac{1}{L_c} \cdot (\theta^+)^3 \cdot N_{col}^{-1} \quad . \tag{5}$$

Here r_e, m are electron classical radius and mass, J_e - electron beam density (when electron beam cross section exceeds positron beam one), L_c - Coulomb logarithm, θ^+ - the angular spread in positron beam, η_e - the ratio of cooling section length to positron ring circumference, N_{col} is an effective number of electron-positron collisions (see Formula (6) below). This formula at $N_{col} = 1$ corresponds only to so called "fast collisions" (see Ref.[5]) and neglects the effects of electron and positron magnetization. So, it is the upper limit for cooling time. For parameters chosen here (see Table 3 below) the Coulomb logarithm decreases with positron velocity decrease in the range $17 \div 8$.

If electrons and positrons are immersed in magnetic field, the collisions between them can repeat few times during one interaction event [3] due to rotation around magnetic field line. The number of such multiturn collisions is equal, by order of magnitude, to

$$N_{col} = \frac{\omega_B \tau_{int}}{2\pi}, \quad \tau_{int} = \min\left\{\frac{l}{v_0}, \frac{\rho_L}{\left\langle\left|\left(\vec{V}^+ - \vec{V}_e\right)_{\parallel}\right|\right\rangle}\right\}. \tag{6}$$

Here τ_{int} is characteristic interaction time, ω_B, ρ_L - the particle Larmor frequency and Larmor radius in magnetic field B, $\vec{V}^+$, $\vec{V}_e$ - particle velocities in the particle rest frame, l - the cooling section lenght. This effect can decrease the cooling time significantly if positron electrostatic acceleration is used (4):

$$N_{col} \sim \sqrt{\frac{2\varepsilon_0}{T_t}} \sim 5 \div 8 N_{col} \sim \sqrt{\frac{2\varepsilon_0}{T_t}} \sim 5 \div 8. \tag{7}$$

Few effects limit equilibrium temperature and life time of the cooled positron beam.

4.1. Multiscattering of positrons in residual gas

Positron beam size increases due to this process with characteristic time

$$\tau_{ms} = \frac{\beta^3\gamma^2}{4\pi Z(Z+1)} \cdot \frac{(\theta)^2}{cr_e^2 n_0 L_z}, \tag{8}$$

$$L_z = \ln(183 \cdot Z^{-1/3}),$$

where Z is atomic number of residual gas atoms.

4.2. Singlescattering of positrons in residual gas

This process limits positron life time, what is equal to

$$\tau_{ss} = \frac{\beta^3\gamma^2}{4\pi Z(Z+1)} \cdot \frac{(\theta^+)^2}{cr_e^2 n_0}, \tag{9}$$

where θ **is aperture scattering angle.**

4.3. Energy exchange between positrons and antiprotons

It is also the same electron cooling mechanism, that transfers energy from positrons to antiprotons or back during their interaction in recombination region. One can neglect this effect in presence of strong electron cooling.

4.4. The generation of positronium

Positron life time is limited also by recombination with electron in cooling region of positron ring, and positron beam intensity decreases due to this recombination with characteristic time, what is analogous to $\bar{p}e^+$ recombination:

$$\tau_{pos} = \frac{N^+}{R_{pos}}, \tag{10}$$

where R_{pos} is given by Formulas (1), (2), if to exchange $V_p \rightarrow V^+$ and to multiply α_r by 4 (technical mass square). One should note, that in e^+e^- recombination parapositronium production prevails, and its life time is very short - 0.125 nsec, or the flight length - 1.25 cm, when particle velocity is about 10^{10} cm/sec. *Ortopositronium* life time is 0.14μsec, and the flight length - 14 m. It means, that cooling section of positron ring is *a source of ortopositronium*, what gives *additional possibilities for physics experiments.*

4.5 Intrabeam scattering (IBS)

In competition with electron cooling this process can define the momentum spread in an intense positron beam [5]:

$$\left(\frac{\Delta p_{\parallel}}{p}\right)^2_{IBS} \sim \frac{n^+}{\beta^3\gamma^3 n_e \theta^+} \cdot \left(\frac{\Delta_{\parallel}}{c}\right)^3, \tag{11}$$

where n_e, n^+ - the densities of the electron beam and the positron one (in laboratory rest frame), $\Delta_{\parallel}$ - the longitudinal velocity spread of electrons in particle rest frame. This effect is negligible practically.

4.6. Equilibrium state

The heating effect, described in p.4.1, is negligible, if $a_0\, \tau_{ee} \rangle\rangle\, \tau_{ms}$ then equilibrium size of the positron beam at low intensity is defined by cooling process.

The cooling of magnitized positrons by magnetized electrons, that takes place in the case under discussion, has some disadvantage compared to heavy particles. The last ones can be cooled down to the longitudinal electron temperature [5], because they do not feel the magnetic field influence. By contrast, magnetized positrons have in equilibrium state nonuniform velocity distribution:

$$T_{\perp}^+ \rightarrow (T_e)_{\perp}, \quad T_{\parallel}^+ \rightarrow (T_e)_{\parallel} \quad . \tag{12}$$

Thus, one can admit

$$V^+ \sim \sqrt{\frac{2(T_e)_{\perp}}{m}} \sim 3 \cdot 10^7 \text{ cm/sec} . \tag{13}$$

5. The positron ring

In proposed scheme the positron ring (Fig.2) has 4 toroidal solenoids and 4 straight ones. The last ones are used for injection/extraction of electrons and positrons, electron cooling of positrons and production of $\bar{p}e^+$ recombination.

The magnetic field strength should be chosen equal to the field in LEAR e-cooler, what is about 600 G.

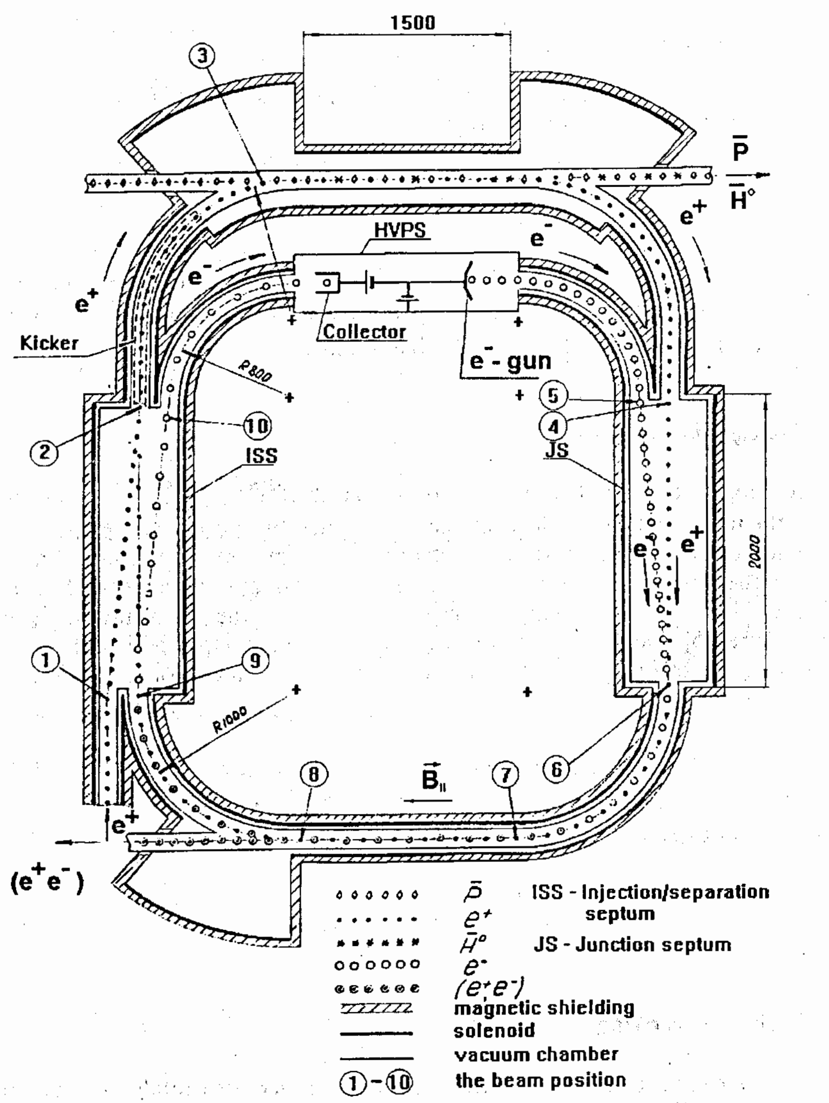

Fig.2. The layout of the positron ring.
ISS - Injection/separation septum, JS - Junction septum,
HVPS - High Voltage Power Supply. All the dimensions are given in mm.

5.1. The electron/positron beams superposition & separation. Positron injection

This problem is complicated enough in presence of a longitudinal magnetic field. The most effective way is, to our opinion, use of centrifugal drift of particles in toroids. The particle drift velocity is directed along toroid axes and equal to [13]

$$\upsilon_{cf} = \frac{\beta^2 \gamma m c^3}{eBR} = \frac{\rho_L}{R} \cdot \beta c, \tag{14}$$

where R is the toroid radius (Fig.3), ρ_L - Larmor radius of the particle. It follows from (14), that a particle displacement, caused by drift, depends only on bending angle in the toroid θ_0 and particle Larmor radius:

$$\Delta_{cf} = \theta_0 \cdot \rho_L \tag{15}$$

and does not depend on bending radius (BR = const in the toroidal coil !). This peculiarity of such a method of a particle displacement is very important and differs it on principle from other methods. Particularly, the magnitude of particle displacement in crossed transverse electrostatic and longitudinal magnetic fields depends on particle transverse coordinate, because particle energy changes after entering in electric field.

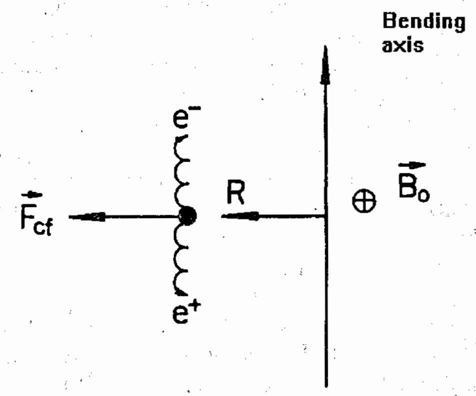

Fig.3. The scheme of centrifugal drift

The centrifugal drift can perturb particle motion and induce some transverse velocity. If entrance in toroidal magnetic field is adiabatic (when the length of the transition region from the straight solenoid field to toroidal one is much larger of Larmor radius ρ_L), such a perturbance is negligible:

$$\Delta V^{+} \le \upsilon_0 \frac{a_0 r}{\rho_L^2} \cdot e^{-r/\rho_L}. \qquad (16)$$

Here r is the radius of solenoid coil, a_0 - the positron beam radius.

If positron drift is compensated with application of transverse bending field, an electron displacement is twice larger: $\Delta_{tot} = 2\Delta_{cf}$.

The same principle is used for positron beam injection. Positrons are generated by some positron source and travel along solenoid magnetic field to the entrance of the positron ring (Fig.2, position 1). Here positron beam is located to the left from central trajectory in the ring and above its median plane (Fig.4,5, pos.1). Then it comes into the septum, what is superposition of longitudinal B and transverse (horizontal) B_h magnetic fields (Fig.5). Here positrons have horizontal displacement to the right

$$\Delta_{septum} = \frac{B_h}{B} \cdot L_{septum} \qquad (17)$$

and come to the position 2 on toroid entrance (see Fig.2,4,5). Then they travel in toroidal magnetic field and additional vertical magnetic field of a *kicker*.

Let's suppose, that this kicker field is directed downwards and it is just equal (by absolute value) to a conventional bending field for positron trajectory radius R (this conventional field must be directed up). Then positrons displace down in agreement with formula (15) and come in the position 3 in median plane. From this point positrons travel along the central trajectory of the ring and do not feel any influence of septum field due to *septum design* (Fig.5).

When singleturn injection of positrons is over, *the kicker field* changes its direction. This procedure seams not too complicated because of long revolution period of positron in the ring (200 nsec for 27 keV positrons). If the switch time of the kicker is equal to 20 nsec, an *induction voltage* on the kicker is about 5 kV.

Now - the electron beam motion. Electrons travel from the gun (Fig.3) to the junction section (Fig.2,5,6, position 5). Here the electron beam is below the median plane and to the right from the central trajectory. In horizontal field of *junction septum* and longitudinal field of solenoid the beam displaces to position 6. If direction of bending field in toroids is agreed with positron motion, electrons are drifting up and come to the central trajectory at position 7 - junction is over! *Electron cooling* of positron occurs between positions 7 and 8. Thereupon electrons displace up again to position 9 in the next toroid, to the right in *injection/separation septum* and come to the collector.

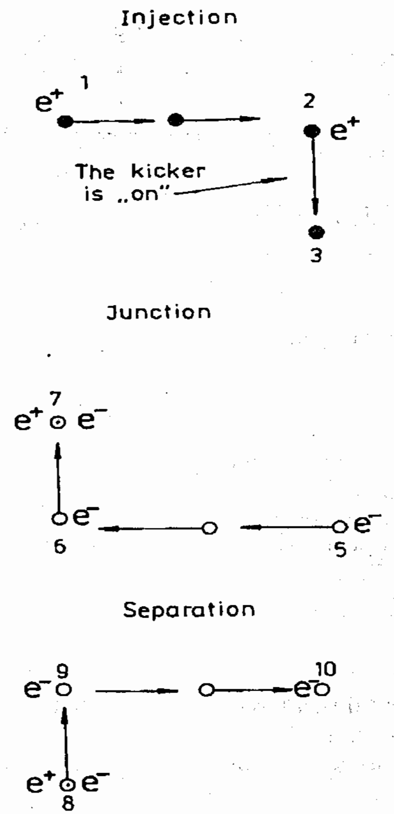

Fig.4. The scheme of particle motion in cross-section plane of the septums

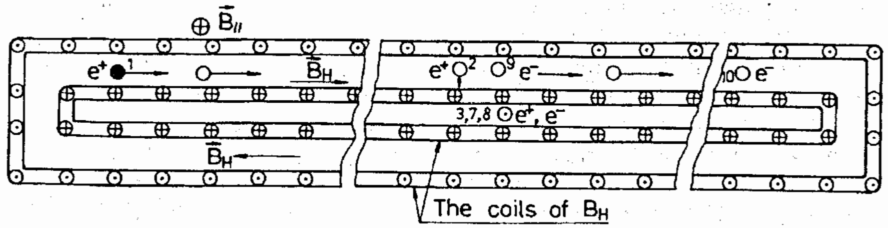

Fig.5. The cross-section of the septum

Table 3.
The general parameters of the positron storage ring

Electron & positron energy	keV	27	0.27
Circumference	m	21.56	
Toroid radius	m	1.0	
Straight section length	m	2×1.5 2×3	
Longitudinal magnetic field	G	600	60
Larmor radius	cm	0.85	
Electron beam			
diameter	mm	3	
beam current density	A/cm^2	1	0.002
Positron beam			
intensity		$1\cdot10^9$	$1\cdot10^8$
current	μA	75	7.5
energy spread of the target	eV	3	
beam diameter	mm	3	
injection angular spread	mrad	10	100
angular spread after cooling	mrad	2	20
Vacuum pressure	Torr	$1\cdot10^{-10}$	$1\cdot10^{-10}$
Characteristic times:			
at injection			
electron cooling	μsec	2	300
positron multiscattering	msec	25	2.5
at equilibrium state			
positron multiscattering	msec	320	32

5.2. The positron motion stability

The proposed focusing system is very similar to "stellarator" one, well known in plasma physics (see, for instance, Ref.[14]). The difference is the significant magnitude of the longitudinal component of the positron momentum. In principle, one can create very precise equilibrium trajectory for single particle - let say, on the axis of the positron beam. However, some disagreement between the momentum of unaxial particle and bending (dipole) magnetic field in toroids always exists. The toroidal magnetic field has also some radial gradient. Both these reasons bring the centrifugal drift, essentially depressed in comparison with the full value (14), when bending field is on. Nevertheless, this slow drift can limit the particle life time in the ring. The method to avoid this problem is known from stellarator experience: one has to superimpose two couples of spiral conductors with opposite current directions on the torus solenoid (Fig.6).

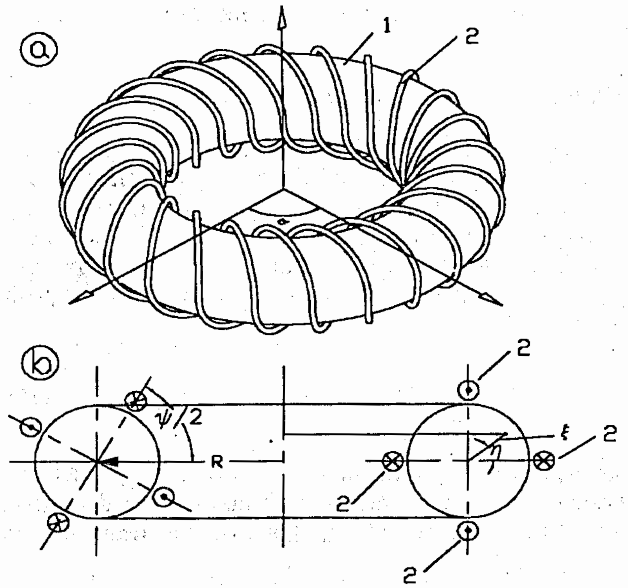

Fig.6 The magnetic system (a) and its cross-section (b). 1–torus coil, 2–spiral winding

In such a solenoid a magnetic field line has the form of a spiral, wrapped around toroidal surface, coaxial with the torus, if the conductor currents generate the quadrupole magnetic field with sufficiently large gradient G (see details in Appendix A). The particle motion is stable in such a field even at some disagreement $\Delta B_\perp$ between the particle momentum p and the bending magnetic field $B_\perp$, if conditions (A.15) of Appendix A are respected. Positrons have additional angular spread because of motion in such a field, equal to

$$\left(\Delta\theta^+\right)^2 \sim 2\left(\Delta\frac{2q}{g}\right)^2 + \left(\frac{2a_0}{\chi R}\right)^2$$
$$\Delta = \frac{\Delta B_\perp}{B_\perp},\ g = \frac{eGR^2}{pc},\ \chi = \frac{R}{\rho_L}, \qquad (18)$$

R - the large radius of the torus, $2\pi q^{-1}$ - the period of the spiral winding, a_0 - positron beam radius.

One can expect, in principle, an appearance of resonance phenomena, similar to ones, which take place in the particle motion in conventional storage rings. However, this problem needs closer examination, which is in progress now. The experience of operation of stellarator machines [14] allows to hope, that an achievement of positron stable motion is possible. One should note also, that positron and electron beam space charge may be a contributary factor for the stability.

5.3. Multiple singleturn injection and storing of positrons

The low intensity of positron source sets one using of positron storing. And only possibility remains in the case of longitudinal magnetic field - to use a storing in longitudinal phase space. The singleturn injection, described in p.5.1. can be used then, together with continuous electron cooling [15]. Such a method needs some radio-frequency accelerating system, but of very modest parameters. Actually, the RF voltage for separatrix, accepting full energy spread of positrons at injection, is

$$V = \frac{\pi T_s}{e} \sim 10 \text{ V}. \tag{19}$$

The analysis shows (see Appendix C), that the phase stability of particle motion in such a magnetic system and rf-accelerating field takes place definitively, if magnetisation condition (B.5) is respected. In this case the transition energy factor is equal to

$$\gamma_{tr} = \frac{R}{2q\rho_L}\left(\frac{GR}{B_0}\right)^2 >> 1 \ . \tag{20}$$

The e^+ storing rate is limited mainly by the source parameters and cooling time value. One example, based on results of Ref.[9,10] is presented in Table 4.

Table 4.

The positron storing rate

Positron energy, keV	27	0.27
e^+ revolution period, μsec	0.21	2.1
Injection repetition rate, sec^{-1}	10^4	10^3
e^+ number per injection cycle	10^4	10^4
Storing time for 10^8, sec	1.0	10.0

6. Vacuum condition

One can see from Table 3, that the requirements imposed on vacuum pressure are not very strict: even at $P = 1\cdot 10^{-10}$ Torr the characteristic time for multiscattering is much larger than electron cooling time at injection. And the situation is even much more better for cooled e^+-beam.

7. The transportation of e^+-beam. Magnetic field variation

So far as source is immersed in longitudinal magnetic field the transportation of positrons from the source to the ring can be performed also in a long solenoid with low magnetic field, about 60 - 200 G. The transportation solenoid can be bent in any necessary direction and it can have some gaps in winding for vacuum pumps, probes etc.

The adiabatic expansion or compression of the solenoid magnetic field in the ring can bring some gain in recombination rate. So, if magnetic field magnitudes are, respectively, B_t - on the positron source, B_{gun} - in the electron gun, B_{cool}, B_{rec} in the cooling and recombination section, the positron equilibrium temperature and positron beam size in the recombination section are equal to

$$T_{rec}^+ = \frac{B_{rec}}{B_{cool}}\cdot (T_e)_\perp \sim \frac{B_{rec}}{B_{gun}} T_{cathode} \ , \qquad \left(a_{rec}^+\right)^2 = \frac{B_t}{B_{rec}}\cdot\left(a_t^+\right)^2 \ . \tag{21}$$

It gives the gain, comparatively to (1), approximately equal to

$$K_{gain} \sim \frac{\sqrt{B_{rec}B_{gun}}}{B_t} \ . \tag{22}$$

It means, that some gain can be obtained, if to increase B_{rec}, B_{gun} and decrease B_t.

8. Conclusion

The level of generation rate, what can be achieved with the proposed scheme, has practical interest: $R \approx 25 \div 10000$ atom/sec in wide range of energy. Some improvements can be done, like expanding of magnetic field in cooling section and its compression in recombination area. They can increase $\overline{H^0}$ yield in few times.

9. Acknowledgements.

We wish to thank J.Bosser, B.Chirikov, M.Charlton , Ya.Derbenev, G.Kulipanov, D.Moehl, L.Rinolfi and V.Volosov for fruitful discussions, J.Eades and L.Montanet for interest to this work.

Appendixes

A. The Spiral Torus Magnetic Field

Let's consider the magnetic field formed by a system of current conductors, which is composed of a torus coil and two couples of spiral wires, superposed on it (see Fig. 6). The torus coil generates the magnetic field with coaxial circle field lines and the strength

$$B_s(r) = B_0 R / r \ , \tag{A.1}$$

where R is the torus large radius, and r, $s = r\alpha$, z - the coordinate system, whose z-axis coincides with the torus axis. The spiral conductors are wound with the step $\lambda = 2\pi R / k >> a$, a- the torus small radius. They generate the rotating quadrupole field

$$B_x = -G(x \sin\psi - z\cos\psi) \ ,$$
$$B_z = G(x\cos\psi + z\sin\psi) \ , \tag{A.2}$$
$$G = 4I / cR^2, \quad x = r - R, \quad \psi = 2ks = 2q\alpha, \quad k = q / R,$$

I - the conductor current, $\psi/2$ - the angle of the spiral rotation of the conductors with coordinate s or α (i.e. the quadrupole field rotates twice faster then conductors).

To analyse the form of magnetic field lines, one can write the line equation

$$\frac{dx}{B_x} = \frac{dz}{B_z} = \frac{ds}{B_s} \ ,$$

what leads (using (A.1), (A.2)) in linear approximation over x, z, to the equations:

$$\frac{dx}{ds} \approx -\frac{G}{B_0}(x\sin\psi - z\cos\psi) \ ,$$
$$\frac{dz}{ds} \approx \frac{G}{B_0}(x\cos\psi + z\sin\psi) \ . \tag{A.3}$$

Multiplying first equation by x, the second one by z and introducing the polar coordinates in the torus cross-section

$$\eta = arctg(z/x) \ , \quad \xi^2 = x^2 + z^2 ,$$

one can obtain:

$$\frac{d\xi^2}{ds} = 2\frac{G}{B_0}\xi^2 \cdot \sin(2\eta - \psi). \tag{A.4}$$

One should use now the new argument $\xi = 2\eta - \psi$. Then

$$\frac{d}{ds} = \frac{d}{d\zeta}\cdot\left(2\frac{d\eta}{ds} - 2k\right), \quad \frac{d\eta}{ds} = \frac{1}{\xi^2}\left(x\frac{dz}{ds} - z\frac{dx}{ds}\right) = \frac{G}{B_0}\cos\xi \ . \tag{A.5}$$

Substitution of formulae (A.5) into equation (A.4) and integration give

$$\xi^2(\zeta) = \frac{C}{q - b\cos\zeta} \ , \quad b = \frac{GR}{B_0} \ , \quad C = const \ . \tag{A.6}$$

It is the equation of the magnetic field line in an implicit form. Nevertheless, one can conclude from this equation, that a point of the magnetic line is confined inside a bounded region of a space, if

$$b < q \ . \tag{A.7}$$

That is the condition of the existence of a confined **magnetic surface**, formed by magnetic line, well known in plasma physics as "the Kruscal - Shafranov condition" [14]. One should note, that at $k \to 0$ the equation (A.6) leads to

$$\xi^2(\eta) = \frac{\xi^2(0)}{\cos 2\eta} \to \infty, \ \text{if} \ \eta \to \left(n + \frac{1}{4}\right)\pi \ .$$

Physically, it means, that such magnetic line goes to infinity, if quadrupole does not rotate.

Let's estimate now an influence of an uniform magnetic field, applied to such spiral torus system along z-axis:

$$B_z^0 / B_0 \equiv h \ . \tag{A.8}$$

Then the second equation in (A.3) receives an additional term in the right hand side. One can combine both equations (A.3) in one, if to introduce the complex function $W(\alpha) = x + iz$. It leads to the equation

$$\frac{dW}{d\alpha} = ibW^* e^{i\psi} + Rh \ . \tag{A.9}$$

The symbol $(\ )^*$ indicates the operation of conjugation.

Let's seek the solution as the sum of fast oscillating and slow varying functions:

$$W(\alpha) = U(\alpha) + A(\alpha)e^{i\psi} \ .$$

After substation in (A.9) and separation of slow and fast parts one can obtain

$$A \approx \frac{b}{2q}U^*, \quad \frac{dU}{d\alpha} = ibA^* + Rh \ . \tag{A.10}$$

The substitution of A magnitude in the second equation for $U(\alpha)$ and integration give

$$U(\alpha) = i\frac{Rh}{Q} + \left(U(0) - i\frac{Rh}{Q}\right)e^{iQ\alpha} \ , \tag{A.11}$$
$$Q = \frac{b^2}{2q} = \frac{1}{2q}\left(\frac{GR}{B_0}\right)^2 .$$

This solution is correct, if the "frequency" Q is small enough:

$$Q << 2q \quad \text{or} \quad b << 2q \ . \tag{A.12}$$

Thus, we are coming again to the condition (A.7) of the confined magnetic surface existence. This surface is slightly distorted by the transverse field (A.8), if

$$\left|\frac{W(\alpha) - W(0)}{W(0)}\right| << 1 \tag{A.13}$$

that leads to the second condition:

$$b >> \sqrt{\frac{qRh}{\xi(0)}} \ . \qquad \text{(A.14)}$$

The conditions (A.7), (A.12) and (A.13) can be combined as following ones:

$$\sqrt{\frac{qRh}{\xi(0)}} << b << 2q \ . \qquad \text{(A.15)}$$

The right hand inequality provides the existence of a confined magnetic surface, the left hand one limits the level of distorting magnetic field.

At such conditions the equations of magnetic field line can be represented by the formula

$$W(\alpha) \approx i\frac{Rh}{Q}(1-e^{iQ\alpha}) + \left(W_0 + \frac{b}{2q}W_0^*\right)e^{iQ\alpha} -$$
$$-i\frac{Rh}{Q}(1-e^{iQ\alpha})\,e^{i\psi} + \frac{b}{2q}W_0^* \cdot e^{i(\psi - Q\alpha)} \ . \qquad \text{(A.16)}$$

At last, two inequalities (A.15) give the condition for q:

$$q >> \frac{Rh}{\xi(0)} \ . \qquad \text{(A.17)}$$

B. The Motion Of A Charged Particle In The Spiral Torus Magnetic Field

Let the particle with the charge e and mass m to be injected in the spiral torus magnetic field described in Appendix A. The particle momentum $\vec{p}$ will be considered here to have at the injection point the direction slightly different with magnetic line one, that is

$$\vec{p} = \{p_x, p_s, p_z\}, \quad p_s \approx |\vec{p}|, \quad p_{x,z} = \theta_{x,z} \cdot p, \quad \theta_{x,z} << 1 \ .$$

To keep the particle on the circular trajectory, coinciding with central magnetic line (the circle of the radius R), one has to apply the transverse magnetic field along z-axis:

$$B_z^0 = -\frac{pc}{eR} \ . \qquad \text{(B.1)}$$

Then the equations of the particle motion, written in coordinates (r, α, z), have the following view:

$$\ddot{r} - r\dot{\alpha}^2 = \frac{e}{\gamma mc}(r\dot{\alpha}B_z - \dot{z}B_\alpha) \ ,$$
$$\frac{1}{r}\cdot\frac{d}{dt}\left(r^2\dot{\alpha}\right) = -\frac{e}{\gamma mc}(\dot{r}B_z - \dot{z}B_r) \ , \qquad \text{(B.2)}$$
$$\ddot{z} = -\frac{e}{\gamma mc}(r\dot{\alpha}B_r - \dot{r}B_\alpha).$$

One can admit in our case, that azimuthal component of the particle velocity is approximately constant and equal to v_0: $v_0 = pc/\gamma m \approx \dot{s} = r\dot{\alpha}$. After substitution of Formulae (A.1), (A.2), (B.1) into equations (B.2) and linearzation over x, z one can write:

$$x'' + x + \chi z' - g(x\cos\psi + z\sin\psi) = -R\Delta \ , \qquad \text{(B.3)}$$
$$z'' - \chi x' - g(x\sin\psi + z\cos\psi) = 0, \qquad \text{(B.4)}$$

where

$$(\ )' = \frac{d}{d\alpha}, \quad \chi = \frac{R}{\rho}, \quad g = \frac{eGR^2}{pc}, \quad \rho = \frac{pc}{eB_0}, \quad \Delta = \frac{\Delta B_z^0}{B_z^0},$$

Δ - some error in setting of the bending magnetic field (B.1). One can restrict the consideration by **the case of strong magnetisation:** $\chi >> 1$. Then the particle travels principally along a spiral magnetic line (A.6), (A.16) and the goal of the analysis is to elucidate the question of the motion stability. In doing so, the magnetic system will be considered to satisfy the condition

$$\chi Q >> 1, \quad \text{or} \quad \frac{eG}{pc} >> \sqrt{\frac{2q}{\rho R^3}}, \qquad \text{(B.5)}$$

i.e. the magnetisation is even more stronger. In this case one can neglect the second term x in the equation (B.3) and transform both equations in the complex form:

$$V(\alpha) = x + iz, \quad V'' - i\chi V' - gV^* e^{i\psi} = -R\Delta, \qquad \text{(B.6)}$$

One can seek the solution as a sum of three components: slow ("betatron") oscillations, analogous to $U(\alpha)$ in (A.11), the oscillations with quadrupole field periodicity $\Delta\alpha = \pi/q$ and, at last, fast rotation of the particle around a magnetic field line with the frequency x:

$$V(\alpha) = U(\alpha) + Ae^{i\psi} + Ce^{i\chi\alpha} \ . \qquad \text{(B.7)}$$

After substitution of this formula into equation (B.10) and averaging over the fast and "quadrupole" oscillations, one can find two equations for $U(\alpha)$ and A:

$$A \approx \frac{b}{2q}U^*, \quad U'' - i\chi U' - gA^* = -R\Delta \ , \qquad \text{(B.8)}$$

$$b \equiv \frac{g}{\chi} = \frac{GR}{B_0} \ .$$

The condition (B.5) is used here essentially. It is easy to see, that first equations in (B.8) and (A.10) coincide. The second one in (B.8) leads (after substitution of A from the first one) to characteristic equation with the roots

$$Q_{1,2} = \frac{\chi}{2} \pm \sqrt{\frac{\chi^2}{4} - \frac{bg}{2q\chi}} \approx \begin{cases} \chi \\ \dfrac{b^2}{2q} \equiv Q \end{cases} \ . \qquad \text{(B.9)}$$

The first value has to be disregarded, because it corresponds to the fast rotation, taken into account already by the third term in (B.7). So, the solution can be written in the form

$$V(\alpha) = U(\alpha) + \frac{b}{2q}U^*(\alpha)\,e^{i\psi} + Ce^{i\chi\alpha} \ ,$$

$$U(\alpha)=\frac{2q\chi}{g^2}\cdot R\Delta+\left(U(0)-\frac{2q\chi}{g^2}R\Delta\right)e^{iQ\alpha}.$$

Expressing of the constants $U(0)$ and C in terms of initial coordinates V_0 and their derivatives leads to the final result:

$$V(\alpha)\approx\frac{1}{\chi Q}R\Delta\left(1-e^{iQ\alpha}\right)+\left(V_0-\frac{b}{2q}V_0^*\right)e^{iQ\alpha}+\frac{R\Delta}{g}(1-e^{-iq\alpha})\,e^{i\psi}+$$
$$+\frac{b}{2q}V_0^*e^{i(\psi-Q\alpha)}-\frac{iV_0'}{\chi}e^{i\chi\alpha}. \qquad \text{(B.10)}$$

Comparison with the expression (A.16) shows, that particle does travel along the magnetic line $W(\alpha)$ (one should mention, that $h/b\equiv\Delta/g$) and rotates around it with amplitude V_0'. The trajectory is stable as long as the conditions (A.15) are respected.

The case of low gradient $g\to 0$ is worthy of attention:

$$V(\alpha)\to i\Delta\rho\alpha+V_0+\frac{iV_0'}{\chi}\left(1-e^{i\chi\alpha}\right).$$

It is so called **"centrifugal drift"**: the particle travels unimpeded along z-axis. One should mention, that **the gradient drift** disappears in our consideration because the condition (B.5) is respected. In opposite case this drift presents, but the method of complex function, used here, is not correct anymore and analysis becomes much more cumbersome.

For application to the electron cooling one merits to find the total transverse velocity of the particle. It's average value is given by the following expression:

$$\overline{\theta^2}\equiv\frac{\overline{\dot{x}^2}+\overline{\dot{z}^2}}{v_0^2}=\frac{1}{R^2}\overline{|V'(\alpha)|^2}\approx\theta_0^2+2\Delta^2\left(\frac{2q}{g}\right)^2+\left(\frac{2a_0}{\chi R}\right)^2. \qquad \text{(B.11)}$$

where $a_0^2=x_0^2+z_0^2$. Therefore, the enhancement of the particle transverse velocity by spiral torus magnetic field is small, if

$$\frac{2q}{\theta_0 R^2}\cdot\Delta<<\frac{eG}{pc}<<\frac{\theta_0}{a_0\rho}. \qquad \text{(B.12)}$$

The results does not change in general, if quadrupole spiral winding is put only on some put of the torus circumference. Then one can write

$$G(\alpha)=\begin{cases}G, & \alpha_{2n}\le\alpha\le\alpha_{2n+1},\\ 0, & \alpha_{2n+1}\le\alpha\le\alpha_{2(n+1)},\end{cases}$$

where $n=0,1,2,\dots N$ - numbers of the quadrupole section. The sectionally smooth function $G(\alpha)$ can be represented in the form of the Fourier series and its harmonics can be combined with exponents $e^{i\psi}$. It leads to some change of the q value, what does not seem dangerous for the trajectory stability.

C. The Particle Phase Dynamics In The Spiral Torus Magnetic Field

One can analyse the particle motion in the ring, described above, and in presence of accelerating rf-voltage, if to find the dependence of particle revolution frequency ω on the particle momentum p. Evidently, it is

$$\Delta\omega=\omega_0\left(\frac{\Delta v_s}{v_s}-\frac{\Delta r(p)}{r_0}\right), \qquad \text{(C.1)}$$

where v_s, Δv_s are the average value of the azimuthal particle velocity and its deviation, r_0, $\Delta r(p)$- the analogous values of the particle trajectory radius. Using the formula (B.10), one can find

$$\Delta r(p)=\overline{x(\Delta)}\approx\frac{R\Delta}{\chi Q}=\frac{R}{\chi Q}\cdot\frac{\Delta p_s}{p_s}.$$

Then, using (C.1), one has

$$\eta_\omega\equiv\frac{p}{\omega}\cdot\frac{d\omega}{dp}=\frac{1}{\gamma^2}-\frac{1}{\chi Q}. \qquad \text{(C.2)}$$

It means, that such a storage ring has the transition energy factor, equal to

$$\gamma_{tr}=\sqrt{\chi Q}, \qquad \text{(C.3)}$$

and $\gamma_{tr}>>1$ under the condition of strong magnetisation (B.5). Therefore, the particle phase dynamics is stable in the ring.

10. References

[1] G.I.Budker, A.N.Skrinsky. Sov.Phys.-Usp. 21, (1978) 277.
[2] H.Poth. Appl.Phys. A 43, (1987) 287-293; CERN-EP/90-04 (1990).
[3] A.S.Artamonov, Ya.S.Derbenev, E.L.Saldin. Part.Accel., 23, 79-92 (1988).
[4] I.N.Meshkov, A.N.Skrinsky. The report on the 3-d Biennial Conf. on Low-Energy Antiproton Physics, September 1994, Bled, Slovenia.
[5] I.N.Meshkov. Particles and Nuclei, v.25, N 6, 1994.
[6] M.Charlton, J.Eades, D.Horvath, R.J.Hughes, C.Zimmermann. Physics Report, v.241, N 2 (1994) 65-117.
[7] M.Steck et al. Proc.of the 3-d European Part.Conf., v.1 (1992) 827 - 829.
[8] J.Bosser, M.Chanel, R.Ley, G.Tranquille. [7], p.p. 845 - 847.
[9] F.Ebel, W.Faust, C.Hahn et al. NIM A272 (1988) 626-628.
[10] J.Paridaens, D.Segers, M.Dorikens and L.Dorikens-Vanpraft, NIM A287 (1990) 359-362.
[11] G.N.Kulipanov, N.A.Mezentzev and A.N.Skrinsky. Rev.Sci.Inst., v.63, N1 (1992) 289-294.
[12] M.Charlton and G.Laricchia.Hyperfine Interactions, 76 (1993) 97-113.
[13] V.Kudelainen, I.Meshkov, R.Salimov: Preprint INP 72-70, Novosibirsk, (1970), translated in CERN-PS/77-08 (1977).
[14] B.V.Chirikov. Sov.Dokladi Akademy Nauk (1967), V.174, №6, 1313-1316.
[15] Heavy Ion Storage Ring Complex K4-K10, A Technical Proposal, Editor G.M.Ter-Akopian, JINR, Dubna (1992) 23-25.

Received by Publishing Department
on March 21, 1995.